ARCHIVES OF MECHANICS
Arch. Mech. **76** (3), 253–275, 2024, DOI: 10.24423/aom.4392

Stokes flow past a contaminated fluid sphere embedded in a porous medium with slip condition

P. K. MEDURI[1)], P. N. L. DEVI[2)]

[1)] *Department of Mathematics, School of Advanced Sciences, VIT-AP University, Amaravati, Andhra Pradesh, India, e-mails: phanikumarmeduri@gmail.com, phani.m@vitap.ac.in (corresponding author)*

[2)] *Department of Mathematics, Institute of Aeronautical Engineering, Dundigal, Hyderabad, 500043, Telangana, India, e-mail: subbusoft2011@gmail.com*

In this paper, Stokes flow past a contaminated fluid sphere embedded in a porous medium is considered using interfacial slip on the boundary. The stream functions and drag are computed analytically. Special cases are deduced for drag force and a satisfactory agreement is reached with available data in the literature. It was observed that in viscous fluid and couple stress fluid cases with an increase in the viscosity ratio, the slip parameter, the porous parameter there is an increase in the values of the drag coefficient for varying different parameters, respectively. Also noticed that coefficient of drag values for a uniform flow of the viscous fluid flow over a contaminated viscous fluid sphere in a porous medium with the slip condition are superior to those of a couple stress fluid (CSF) flow.

Key words: couple stress fluid (CSF), viscous fluid, surfactant, slip condition, drag force, porous medium.

1. Introduction

The study of fluid flow through porous medium is very important in many areas of science and technology including geophysical fluid dynamics, chemical processing industry, petroleum industry, solidification, recovery of the crude oil, ground water recharge, aquifers, oil technology waste treatment, biology, reaction engineering, soil science and separation science as mentioned in Kumar *et al.* [1], Srinivasacharya and Ramana Murthy [2] and Pavlovskaya *et al.* [3].

Brinkman [4] evaluated the viscous force exerted by a flowing fluid on a dense swarm of particles by introducing modified Darcy's equation for the porous medium, which is commonly known as the Brinkman equation. Partha *et al.* [5] described the impact of tangential stresses developed in the porous

medium because of the stress jump boundary conditions observed in spherical shells. Further the Brinkman equation was used to govern the flow inside the porous medium. Radhika and Iyengar [6] critically analyzed the influence of stresses, drag on spherical shells and bodies having porous structure. The effect of various flow parameters on drag was determined numerically. Alemayehu and Krishnamacharya [7] discussed the couple stress fluids passing in a peristaltic motion due to distribution of a solute in a porous medium under a slip condition. The well-known Taylor principle was used to obtain a closed form solution for the distribution coefficients. Kumar and Mohan [8, 9] in their works discussed the heated layer of couple stress fluid due to the thermo-solutal convection method, which affects the uniform flow of the vertical magnetic field and vertical rotation on the porous fluid flow. Agoor and Eldabe [10] studied the Rayleigh–Taylor instability growth rate in a porous medium for the non-Newtonian Casson fluid with couple stress. Nagaraju *et al.* [11] investigated the behaviour of CSF flow between two concentric rotating vertical porous cylinders subjected to a radial magnetic field.

The solutions accounting for the effects of various control parameters on velocity profiles and temperature distributions were obtained. Rudraiah *et al.* [12] studied the impact of the dispersion coefficient on the porous parameter and the couple stress parameter. Their findings make it obvious that the dispersion coefficient rises with the porous parameter while decreasing with the couple stress parameter. Hassan *et al.* [13] work investigated the influence of temperature-dependent density on extremely ignitable CSF passed through a channel in a steady state by using the Adomian Decomposition Method (ADM). Howle *et al.* [14] work described the effect of convection on porous flows having ordered and disordered patterns, solved by a modified shadow graphic technique. Srinivasacharya and Prasad [15, 16] studied the creeping motion of a porous sphere passing through the center of spherical container with the stress jump boundary condition. They extended the work with the same conditions on a porous approximate sphere. In both the studies, inside and outside flow motions were analyzed with the Brinkman condition. Deo *et al.* [17] reported on drag force effects on a fluid sphere having a porous structure. The Brinkman and Stokes equations were used to study the fluid outside and inside the sphere to numerically analyze the stream function. Widodo *et al.* [18] work reported the nano-fluid through porous spheres when mixed convection conditions were present. The impact of magnetic and convectional characteristics on velocity and temperature profiles was examined using the Keller–Box scheme. Selvi *et al.* [19] investigated the flow around a Reiner–Rivlin non-Newtonian liquid particle with a Newtonian liquid shell in a permeable medium employing Brinkman, Stokes, and Reiner–Rivlin equations, providing analytical solutions and exploring the drag force dependence on permeability, the viscosity ratio, and a dimensionless parameter.

Few applications of contaminated fluid drop are in nuclear power plants, chemical reactors, petroleum refining equipment, sediment and pollutant transport processing in aquatic environment as mentioned in monographs of SADHAL *et al.* [20]. LEE *et al.* [21] explored the motion of a sphere near a fluid-fluid interface, deriving solutions for point force, extending to higher-order terms for solid sphere motion using reflections, and calculating drag force, hydrodynamic torque, and rotational motion for different cases and viscosity ratios. OGUZ and SADHAL [22] have examined the fluid dynamics of moving drops with soluble surfactants and insoluble impurities, proposing a two-impurity model to address experimental discrepancies, utilizing semi-analytical analysis for weakly inertial flows and achieving good agreement with data, including a novel analytical expression for the drag force in cases involving only insoluble surfactants. WASAN [23] have identified a new mechanism for the stabilization of foam and emulsion films via the presence of such ordered microstructures inside the films. The lifetimes of foams or emulsions with stratifying films are observed to be much longer. SABONI *et al.* [24] developed a numerical equation and used it to analyze the effect of interface contamination and the flow system on the concentration profiles, inside and outside a fluid sphere for different ranges of the Reynolds number. MURTHY and KUMAR [25] considered the viscous flow through the contaminated fluid sphere with no slip condition and calculated the shear stress and resistance on the surface.

NAVIER [26] introduced the slip boundary condition which assumes that the amount of slip is proportional to the shear rate in the fluid at the solid surface and the slip length is defined as the distance from the fluid-solid interface to where the linearly extrapolated tangential velocity vanishes. VINOGRADOVA [27] analysed the apparent slip of fluids at the hydrophobic interface and concluded that this slippage was caused both by a less viscous oil film close to the solid interface and, possibly, by an air film at the solid/liquid interface. NG [28] explored the impact of wall slip on hydrodynamic dispersion in pressure-driven flows, particularly when slip lengths are unequal or involve phase exchange with the wall, can either reduce or reverse the decreasing effect on dispersion observed in a basic case, affecting convection speed and dispersity. FENG *et al.* [29] examined the hydrodynamic drag force on a small viscous sphere with an interfacial slip. Using a singular perturbation method, they derived an analytical expression for the drag force coefficient and observed a significant reduction in the drag force due to interfacial slip. The monographs of HAPPEL and BRENNER [30] and MICHAELIDES [31] have explained in detail about the fluid sphere, its size and shape, and applications of fluid sphere models in industry. Also, the slip boundary condition at the interface of a fluid sphere is described (page 81) by MICHAELIDES [31]. MURTHY and KUMAR [32] have obtained the drag value and the vorticity function for an impervious sphere for intermedi-

ate Reynolds numbers with a slip on its surface using the Homotopy Analysis Method. It was observed that the vorticity diffusion and the wake size beyond the sphere are rising with a rise in Reynolds number. Devi and Kumar [33, 34] have obtained an exact solution for CSF flow beyond a fluid drop filled with a CSF using slip and illustrated the drag force analytically. Also, extended the work over a partially contaminated fluid sphere with the same condition. Devi and Kumar [35] have addressed oscillatory couple stress fluid flow on a contaminated fluid sphere with slip on a boundary. Analytic methods were used to obtain the stream function and drag force. Lakshmi and Kumar [36] have obtained an analytical solution for drag with uniform flow of micropolar fluid past a fluid sphere. An exact solution of a micropolar fluid flow past a contaminated fluid sphere with the slip condition was obtained by Lakshmi and Kumar [37].

Debye and Bueche [38] extended Einstein's theory for impermeable spheres to calculate intrinsic viscosity, diffusion, and a sedimentation rate of polymers, substituting a coiled polymer molecule as a hindrance to liquid flow, with the resulting shielding determining the exponent in the exponential relation between intrinsic viscosity and molecular weight, emphasizing the indirect and polymer-specific nature of this relationship. Danov *et al.* [39] addresses the slow motion of a spherical particle in viscous liquid, exploring Brenner and Leal's theory on surface diffusivity and providing insights into the "drag-out problem", revealing a significant decrease in the surface diffusion coefficient with increasing surface viscosity for various contact angles. Cristini *et al.* [40] introduced a three-dimensional boundary integral algorithm with adaptive surface discretization for accurately simulating drop breakup in viscous flows, applied to study breakup under shear flow and buoyancy with comparisons to experimental observations. Stone *et al.* [41] studied electro-kinetic transport phenomena encountered in most microfluidic devices. Electro-osmotic flow is one of the popular electro-kinetic transport phenomena of microfluidic flow and refers to the movement of ionized liquids in the channel, which is induced by an external electric field.

The available literature focused on couple stress fluids, porous medium and contaminated fluid spheres on different geometries with slip and without slip conditions. The mentioned works have not addressed much on the porous medium of a CSF (non-Newtonian fluid) flow on a surfactant fluid sphere with the slip condition. The present work mainly focuses to give an analytical solution for geophysical applications found in different categories of flows like viscous fluid flow past a contaminated fluid sphere fixed in a porous medium and couple stress fluid flow past a contaminated fluid sphere fixed in a porous medium. Hence, the combination of the CSF flow over contaminants fluid sphere is a new study. This study fills the research gap and it shows new directions for the researchers to work more in this area.

The paper is organized as follows: In Section 2, we consider uniform flow of viscous fluid flow over a contaminated viscous fluid sphere in a porous medium. In Section 3, we analyze uniform flow of the CSF flow over a contaminated CSF sphere in a porous medium.

2. Uniform flow of viscous fluid over a contaminated viscous fluid sphere in a porous medium:

2.1. Formulation of the problem

Consider a uniform flow of the viscous fluid over a contaminated viscous fluid sphere which is fixed in a porous medium. The outside fluid and inside fluid are immiscible. The fluid sphere is assumed to be non-deformed, with a small size as mentioned in monographs of SADHAL *et al.* [20] and MICHAELIDES [31]. The flow is two dimensional, steady, axisymmetric and not compressible with no body forces. The surfactants (contamination) in the flow accumulate at the rear end forming a cap region. The thickness of contamination is uniform and small. The extension of contamination region is mentioned as x_0 which is a varying point in between -1 to 1. The region which is contaminated is known as cap region $(x_0 < x \leq 1)$ and the remaining portion $(-1 < x \leq x_0)$ is no cap region. The geometry is given in Fig. 1.

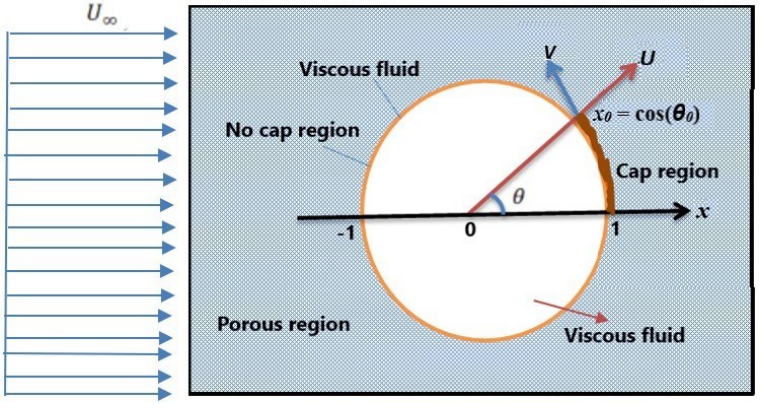

FIG. 1. Flow geometry of viscous fluid past a contaminated viscous fluid sphere embedded in a porous medium.

We assume that the Brinkman model governs the region outside the flow with a porous medium.

The equation of continuity is

$$\nabla \bar{q} = 0. \tag{2.1}$$

The field equation that determines the internal flow of the viscous fluid flow is as follows:

$$\nabla^2 \bar{q} = \left(\frac{1}{\mu_i}\right) \nabla P, \tag{2.2}$$

the momentum equation of the outer region with the porous region is

$$\nabla^2 \bar{q} - \left(\frac{\Gamma_1}{a}\right)^2 \bar{q} = \frac{1}{\mu_e} \nabla P. \tag{2.3}$$

Here, P is hydrostatic pressure at any point, ρ is fluid density, $\bar{q}$ is fluid velocity, μ_e is external fluid viscosity, μ_i is internal fluid viscosity, μ is coefficient of viscosity, Γ_1 is root of the equations for the given porous function, k is the permeability of the porous medium, $U_\infty$is velocity at infinity.

Due to the geometrical shape of the present problem, we choose a spherical coordinate system (R, θ, φ) for reference. The scale factors for the system are $h_1 = 1$, $h_2 = R$, $h_3 = R \sin\theta$. "The spherical coordinate system with the origin at the center of the sphere and Z-axis along the flow direction as considered" [34].

In the axisymmetric flow, velocity components U, V are expressed as:

$$U(R,\theta) = \frac{1}{R^2 \sin\theta} \frac{\partial \Psi}{\partial \theta}, \quad V(R,\theta) = \frac{-1}{R \sin\theta} \frac{\partial \Psi}{\partial R}, \quad \bar{q} = \nabla \times \frac{\Psi \bar{e}_\theta}{R^2 \sin\theta}. \tag{2.4}$$

Here

$$\Psi = \begin{cases} \Psi_i, & R < a, \\ \Psi_e, & R \geq a. \end{cases}$$

Eliminating pressure P in Eq. (2.3) and using non-dimensional parameters:

$$\begin{aligned} &R = ar, \quad \Psi = \psi U_\infty a^2, \quad P = p\frac{U_\infty \mu}{a}, \quad E_0^2 = \frac{E^2}{a^2}, \\ &U = uU_\infty, \quad V = vV_\infty, \quad \text{porosity parameter } \Gamma_1^2 = \frac{a^2}{k}, \end{aligned} \tag{2.5}$$

reduces Eq. (2.2) and Eq. (2.3) to:

$$E^4 \psi_i = 0, \tag{2.6}$$

$$E^2 [E^2 - \Gamma_1^2] \psi_e = 0, \tag{2.7}$$

where

$$E^2 \equiv \frac{\partial^2}{\partial r^2} + \frac{1}{r^2} \frac{\partial^2}{\partial \theta^2} - \frac{\cot\theta}{r^2} \frac{\partial}{\partial \theta}.$$

When $x = \cos\theta$, we get,

$$E^2 \equiv \frac{\partial^2}{\partial r^2} + \frac{1 - x^2}{r^2} \frac{\partial^2}{\partial x^2}.$$

The solutions of ψ Eqs. (2.6), (2.7) which are regular for outside no-cap and cap regions, inside no-cap and cap regions are represented as [25]:

$$\psi'_e(r,x) = \begin{cases} f_{en}(r)G_2(x) & \text{for } -1 < x \le x_0 \text{ (no cap region)}, \\ f_{ec}(r)G_2(x) & \text{for } x_0 < x \le 1 \text{ (cap region)}, \end{cases} \tag{2.8}$$

$$\psi'_i(r,x) = \begin{cases} f_{in}(r)G_2(x) & \text{for } -1 < x \le x_0 \text{ (no cap region)}, \\ f_{ic}(r)G_2(x) & \text{for } x_0 < x \le 1 \text{ (cap region)}. \end{cases} \tag{2.9}$$

The solutions of viscous fluid flow over a contaminated viscous fluid sphere in a porous medium are given by Eqs. (2.8) and (2.9) which are regular for outside flow of no-cap and cap regions are $(f_{en}(r)\,\&\,f_{ec}(r))$ and for inside flow of no-cap and cap regions are $(f_{in}(r)\,\&\,f_{ic}(r))$:

$$f_{en}(r) = \left(\frac{f_1}{r} + r^2 + g_1\sqrt{r}K_{\frac{3}{2}}(\Gamma_1 r)\right), \tag{2.10}$$

$$f_{in}(r) = (f_2 r^2 + g_2 r^4), \tag{2.11}$$

$$f_{ec}(r) = \left(\frac{f_3}{r} + r^2 + g_3\sqrt{r}K_{\frac{3}{2}}(\Gamma_1 r)\right), \tag{2.12}$$

$$f_{ic}(r) = (f_4 r^2 + g_4 r^4), \tag{2.13}$$

"where $K_{\frac{3}{2}}(x)$ and $I_{\frac{3}{2}}(x)$ are Modified Bessel's functions of order $\frac{3}{2}$ and $G_2(x) = \frac{1}{2}(1-x^2)$ is the Gegenbauer polynomial of order 2" [36].

In a cap region $f_4 = g_4 = 0$, i.e., $\psi'_{ic} = 0$.

The parameters f_1, g_1, f_2, g_2, f_3, g_3 in Eqs. (2.10)–(2.13) are obtained by implementing the following boundary conditions (BC's) Eqs. (2.14)–(2.17).

(i) Regularity conditions:

$$\begin{aligned} &\text{a) } \lim_{r\to\infty} \psi'_e = \tfrac{1}{2}r^2\sin^2\theta \text{ (outside the region)}, \\ &\text{b) } \lim_{r\to 0} \psi'_i = \text{Finite (inside the region)}. \end{aligned} \tag{2.14}$$

(ii) Impermeability condition: On the boundary normal velocity is zero,

$$\psi'_{en} = \psi'_{ec} = \psi'_{in} = \psi'_{ic} = 0 \quad \text{on } r = 1 \text{ and } (-1 \le x \le 1). \tag{2.15}$$

(iii) Slip condition: "The tangential velocity is directly proportional to the tangential stress along the surface" [30, 31, 36], i.e.,

$$\tau_{r\theta e} = \vartheta(V_{\theta e} - V_{\theta i}), \quad \text{where } \vartheta \text{ is the sliding friction and } (-1 \le x \le 1), \tag{2.16}$$

where $V_{\theta e}$, $V_{\theta i}$ stands for external and internal tangential velocities respectively.

(iv) Shear stress continuous is continuous at the surface of the fluid sphere, i.e.,

$$\tau_{r\theta e} = \tau_{r\theta i} \quad (-1 \le x \le x_0). \tag{2.17}$$

The boundary conditions are from [20, 30, 31].

2.2. Elucidation of the problem

Using BC's (2.14)–(2.17) in Eqs. (2.10)–(2.13), the system of equations was obtained:

$$\begin{aligned}
&f_1 = -(1+g_1'),\\
&f_2 = -g_2,\\
&f_3 = -(1+g_3'),\\
&f_1(s+4) + g_1'(\Gamma_1^2 + 2 + (s+2)\Delta_1(\Gamma_1)) + 2sf_2 + 4sg_2 = 2+2s,\\
&f_3(s+4) + g_3'(\Gamma_1^2 + 2 + (s+2)\Delta_3(\Gamma_1)) = 2s+2,\\
&4f_1 + g_1'(2+\Gamma_1^2 + 2\Delta_1(\Gamma_1)) + 2\mu f_2 - 4\mu g_2 = 2,
\end{aligned} \tag{2.18}$$

where $g_1' = g_1 K_{\frac{3}{2}}(\Gamma_1)$, $g_3' = g_3 K_{\frac{3}{2}}(\Gamma_1)$, slip parameter $(s) = \frac{\vartheta a}{\mu}$, viscosity ratio $(\mu) = \frac{\mu_i}{\mu_e}$.

Solving the system of Eqs. (2.18) analytically, resulted to:

$$\begin{aligned}
&g_1' = \frac{(3s+6)n_2' - 6m_2'}{m_1'n_2' - m_2'n_1'}, \quad g_2 = \frac{6m_1' - (6+3s)n_1'}{m_1'n_2' - m_2'n_1'}, \quad g_3' = \frac{3s+6}{m_3'},\\
&m_1' = [-s-2+\Gamma_1^2 + (2+s)\Delta_1(\Gamma_1)], \quad m_2' = [2s],\\
&n_1' = [-2+\Gamma_1^2 + 2\Delta_1(\Gamma_1)], \quad n_2' = [-6\mu],\\
&m_3' = [-s-2+\Gamma_1^2 + (2+s)\Delta_3(\Gamma_1)],
\end{aligned} \tag{2.19}$$

where $\Delta_1(\Gamma_1) = \frac{1+\Gamma_1+\Gamma_1^2}{1+\Gamma_1}$ (no-cap region related), $\Delta_3(\Gamma_1) = \frac{1+\Gamma_1+\Gamma_1^2}{1+\Gamma_1}$ (cap region related).

Thus, outside and inside flow stream functions are found.

2.3. Drag force evaluation

A fluid sphere submerged in a viscous fluid experiences drag force, which is equal to

$$D_{g1} = 2\pi a^2 \int_{\theta=0}^{\pi} [\tau_{rr}\cos\theta - \tau_{r\theta}\sin\theta]_{r=1}\sin\theta\, d\theta. \tag{2.20}$$

Here $\tau_{rr} = -P + 2\mu_e \frac{\partial U}{\partial r}$, $\tau_{r\theta} = \mu_e\big[\frac{1}{r}\frac{\partial U}{\partial \theta} + \frac{\partial V}{\partial r} - \frac{V}{r}\big]$.

Substitution and simplification give, the drag force in terms of a cap angle as:

$$
\begin{aligned}
(2.21)\quad D_{g1} = -2\pi a\mu_e U_\infty \Bigg\{ & \left[\Gamma_1^2 - \frac{\Gamma_1^2}{2} f_1 + 4f_{en}(1) - 2f'_{en}(1)\right]\left[\frac{x_0^3}{3} + \frac{1}{3}\right] \\
& + \left[\Gamma_1^2 - \frac{\Gamma_1^2}{2} f_3 + 4f_{ec}(1) - 2f'_{ec}(1)\right]\left[\frac{1}{3} - \frac{x_0^3}{3}\right] \\
& + [-f''_{en}(1) + 2f'_{en}(1)]\left[\frac{x_0}{2} - \frac{x_0^3}{6} + \frac{1}{3}\right] \\
& + [f_{en}(1)]\left[\frac{x_0^3}{3} - x_0 - \frac{2}{3}\right] + [-f''_{ec}(1) + 2f'_{ec}(1)]\left[\frac{1}{3} - \frac{x_0}{2} + \frac{x_0^3}{6}\right] \\
& + [f_{ec}(1)]\left[-\frac{2}{3} - \frac{x_0^3}{3} + x_0\right]\Bigg\}.
\end{aligned}
$$

The values in Eqs. (2.10) and (2.12) are taken on R.H.S. for computation Eq. (2.21).

When $x_0 = -1$, contaminated fluid sphere reduces to a solid sphere. Then drag Eq. (2.21) becomes:

$$
\begin{aligned}
(2.22)\quad D_{g1} = -2\pi a\mu_e U_\infty \Bigg\{ & \left[\frac{2}{3}\right]\left[\Gamma_1^2 - \frac{\Gamma_1^2}{2} f_3 + 4f_{ec}(1) - 2f'_{ec}(1)\right] \\
& + \left[\frac{2}{3}\right][-f''_{ec}(1) + 2f'_{ec}(1)] - \left[\frac{4}{3}\right][f_{ec}(1)]\Bigg\}.
\end{aligned}
$$

Substituting values from Eq. (2.19) and simplifying we get,

$$
(2.23)\quad D_{g1} = 2\pi a\mu_e U_\infty \left[\frac{(\Gamma_1^2 + 3\Gamma_1 + 3)s + \Gamma_1^3 + 3\Gamma_1^2 + 6\Gamma_1 + 6}{s + \Gamma_1 + 3}\right].
$$

When the slip parameter $(s) \to \infty$, we get no slip condition, then the drag is

$$
(2.24)\quad D_{g1} = 2\pi a\mu_e U_\infty [\Gamma_1^2 + 3\Gamma_1 + 3].
$$

When there is no porosity, i.e., $\Gamma_1 = 0$, then we get the drag force for a solid sphere with no slip condition as

$$
(2.25)\quad D_{g1} = 6\pi a\mu_e U_\infty,
$$

which matches with the results of [17, 30, 42].

When $x_0 = 1$, contaminated fluid sphere reduces to a fluid sphere. Then drag Eq. (2.21) becomes

$$
\begin{aligned}
(2.26)\quad D_{g1} = -2\pi a\mu_e U_\infty \Bigg\{ & \left[\frac{2}{3}\right]\left[\Gamma_1^2 - \frac{\Gamma_1^2}{2} f_1 + 4f_{en}(1) - 2f'_{en}(1)\right] \\
& + \left[\frac{2}{3}\right][-f''_{en}(1) + 2f'_{en}(1)] - \left[\frac{4}{3}\right][f_{en}(1)]\Bigg\}.
\end{aligned}
$$

Substituting the values from Eq. (2.19) and simplifying we get the drag as

$$D_{g1} = 2\pi a\mu_e U_\infty \Gamma_1^2 \left[\frac{s(3\mu\Gamma_1^2+9\mu\Gamma_1+9\mu+\Gamma_1^3+3\Gamma_1^2+6\Gamma_1+6)+3\mu\Gamma_1^3+9\mu\Gamma_1^2+18\mu\Gamma_1+18\mu}{\Gamma_1^2 s(3\mu+\Gamma_1+3)+9\mu\Gamma_1^2+3\mu\Gamma_1^3}\right]. \tag{2.27}$$

When slip parameter $(s) \to \infty$, we get no slip condition, then drag is

$$D_{g1} = 2\pi a\mu_e U_\infty \left[\frac{3\mu(\Gamma_1^2+3\Gamma_1+3)+\Gamma_1^3+3\Gamma_1^2+6\Gamma_1+6}{3\mu+\Gamma_1+3}\right]. \tag{2.28}$$

With the assumption of no porosity,

$$D_{g1} = 2\pi a\mu_e U_\infty \left[\frac{9\mu+6}{3\mu+3}\right]. \tag{2.29}$$

With the viscosity ratio $\mu \to \infty$, we get the drag force for a solid sphere with no slip condition as

$$D_{g1} = 6\pi a\mu_e U_\infty, \tag{2.30}$$

which matches with the results of [17, 30, 42].

Now the coefficient of the drag (C_D) is computed as

$$C_D = \frac{D_{g1}}{\frac{1}{2}\pi\rho U_\infty^2 a^2} = \frac{\pi\mu_e U_\infty a\Gamma_1^2(-2-g_1'-g_3').}{\frac{1}{2}\pi\rho U_\infty^2 a^2}. \tag{2.31}$$

When $s \to \infty$, $\mu \to \infty$, and $\Gamma_1 = 0$, we get

$$C_D = -\frac{24}{Re}, \quad \text{with } Re = \frac{(2a)\rho U_\infty}{\mu_e}, \tag{2.32}$$

which matches with the coefficient of the drag for a solid sphere without a slip condition [30].

3. Uniform flow of the CSF flow over a contaminated CSF sphere in a porous medium

3.1. Problem formulation

The equations of motion characterize a CSF flow as given by STOKES [43]:

$$\frac{\partial\rho}{dt} + \rho\nabla(\bar{q}) = 0, \tag{3.1}$$

$$\rho\frac{d\bar{q}}{dt} = \rho\bar{f} + \left(\frac{1}{2}\right)\nabla\times(\rho\bar{C}) + \nabla(\tau^{(s)}) + \left(\frac{1}{2}\right)\nabla\times(\bar{M}), \tag{3.2}$$

where ρ is density of the fluid, $\tau^{(s)}$ is the symmetric part of the force stress tensor, $\bar{M}$ is the couple stress tensor, $\bar{f}$, $\bar{C}$ are the body force per unit mass and the body couple per unit mass, respectively.

The couple stress tensor m_{ij} that arises in the theory has the linear constitute relation:

$$m_{ij} = \left(\frac{1}{3}\right) m\delta_{ij} + 4\eta\omega_{ji} + 4\eta'\omega_{ij}, \tag{3.3}$$

where ω_{ij} is the spin tensor, η, η' are the couple stress viscosity coefficients with $|\eta'| \leq \eta$ and $\delta_{i,j}$ denotes the Kronecker symbol

$$\delta_{i,j} = \begin{cases} 1, & i = j, \\ 0, & i \neq j. \end{cases}$$

Consider a uniform flow of CSF over a contaminated CSF sphere which is fixed in a porous medium with the Brinkman model, a flow is uniform far from the body. The outside fluid and inside fluid are immiscible. The fluid sphere assumed as non-deformed. Also assumed the size of it to be very small as mentioned in monographs of SADHAL *et al.* [20] and MICHAELIDES [31]. The flow is presumed incompressible, steady and axi-symmetric without body forces. The work geometry is given in Fig. 2.

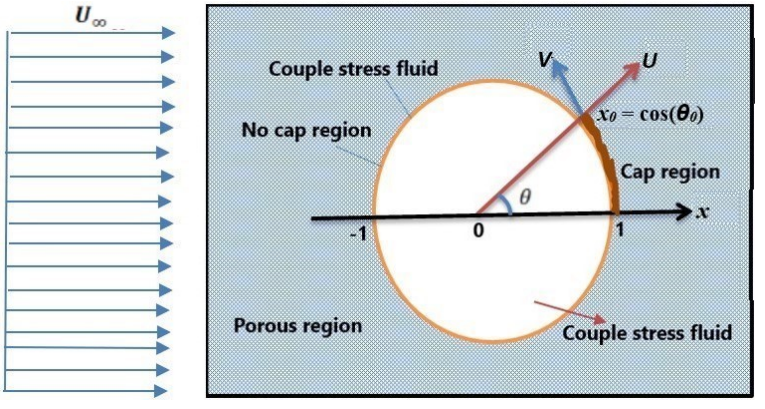

FIG. 2. Flow geometry of CSF past a contaminated CSF sphere embedded in a porous medium.

The Brinkman's equation of a porous medium is taken as:

$$\nabla^2\bar{q} - \left(\frac{\Gamma_1}{a}\right)^2 \bar{q} = \frac{1}{\mu_e}\nabla P,$$

and the CSF equation in absence of body forces is

$$\rho\frac{d\bar{q}}{dt} = -\nabla P + \mu(\nabla\times\nabla\times\bar{q}) - \eta(\nabla\times\nabla\times\nabla\times\nabla\times\bar{q}). \tag{3.4}$$

With Eq. (2.4) and eliminating the pressure P the momentum equation for a dual flow of non-Newtonian fluid past a fluid sphere embedded in a porous medium is given by:

$$E^2[E^2-\delta_1^2][E^2-\Gamma_1^2]\psi = 0, \tag{3.5}$$

where the porosity parameter $\Gamma_1^2 = \frac{a^2}{k}$ and the couple stress parameter $\delta_1^2 = \frac{\mu a^2}{\eta}$, with $x = \cos\theta$, $E^2 \equiv \frac{\partial^2}{\partial r^2} + \frac{1-x^2}{r^2}\frac{\partial^2}{\partial x^2}$.

The solutions of Eq. (3.5) for the outer region (ψ_e'') and for the inner region (ψ_i'') are assumed in the form:

$$\begin{aligned}\psi_{en}''(r,x) &= f_{en}(r)G_2(x)\\ &= \left(\frac{b_1}{r} + r^2 + c_1\sqrt{r}K_{\frac{3}{2}}(\Gamma_1 r) + d_1\sqrt{r}K_{\frac{3}{2}}(\delta_1 r)\right)G_2(x),\end{aligned} \tag{3.6}$$

$$\psi_{in}''(r,x) = f_{in}(r)G_2(x) = (b_2r^2 + c_2r^4 + d_2\sqrt{r}I_{\frac{3}{2}}(\delta_1 r))G_2(x), \tag{3.7}$$

$$\begin{aligned}\psi_{ec}''(r,x) &= f_{ec}(r)G_2(x)\\ &= \left(\frac{b_3}{r} + r^2 + c_3\sqrt{r}K_{\frac{3}{2}}(\Gamma_1 r) + d_3\sqrt{r}K_{\frac{3}{2}}(\delta_1 r)\right)G_2(x),\end{aligned} \tag{3.8}$$

$$\psi_{ic}''(r,x) = f_{ic}(r)G_2(x) = (b_4r^2 + c_4r^4 + d_4\sqrt{r}I_{\frac{3}{2}}(\delta_1 r))G_2(x). \tag{3.9}$$

In a cap region $b_4 = c_4 = d_4 = 0$ and hence, $\psi_{ic}'' = 0$. The parameters b_1, c_1, d_1, b_2, c, d_2, b_3, c_3, d_3 in Eqs. (3.6)–(3.9) are obtained by implementing the following boundary conditions:

(i) Regularity conditions:

$$\begin{aligned}&\text{a) } \lim_{r\to\infty}\psi_e'' = \tfrac{1}{2}r^2\sin^2\theta \quad \text{(outside the region)},\\ &\text{b) } \lim_{r\to 0}\psi_i'' = \text{Finite (inside the region)}.\end{aligned} \tag{3.10}$$

(ii) Impermeability condition: on the boundary normal velocity is zero

$$\psi_{en}'' = \psi_{ec}'' = \psi_{in}'' = \psi_{ic}'' = 0 \quad \text{on } r = 1 \quad (-1 \le x \le 1). \tag{3.11}$$

(iii) Slip condition: "The tangential velocity is directly proportional to the tangential shear along the clear surface" [30, 31], i.e.,

$$\tau_{r\theta e} = \vartheta(V_{\theta e} - V_{\theta i}) \quad (-1 \le x \le 1), \tag{3.12}$$

where $V_{\theta e}$, $V_{\theta i}$ stands for external and internal tangential velocities, respectively.

(iv) Shear stress continuous: at crossing the surface of the fluid sphere, i.e.,

$$\tau_{r\theta e} = \tau_{r\theta i} \quad (-1 \le x \le x_0). \tag{3.13}$$

(v) Type A condition: vanishing of the couple stress on the boundary. In terms of a stream function

$$\left(\frac{\partial[E^2\psi]}{\partial r}\right) = \left(e + \frac{1}{r}\right)E^2\psi \quad (-1 \le x \le 1), \tag{3.14}$$

where $e = \frac{\eta'}{\eta}$ with $(\eta' \neq \eta)$, here η, η' is couple stress viscosity coefficients.

Using the BC's (3.10)–(3.14) in Eqs. (3.6)–(3.9) the following system of equations is obtained:

$$\begin{aligned}
&b_1 + c_1' + d_1' = -1,\\
&b_2 + c_2 + d_2' = 0,\\
&b_3 + c_3' + d_3' = -1,\\
&-(6+s)b_1 + d_1'\left(-\delta_1^2 - 4 - (2+s)\Delta_1(\delta_1) + \frac{\delta_1^4}{\lambda^2}\right)\\
&\qquad + c_1'\left(-\Gamma_1^2 - 4 - (2+s)\Delta_1(\Gamma_1) + \frac{\Gamma_1^4}{\lambda^2}\right)\\
&\qquad - 2sb_2 - 4sc_2 + d_2's\Delta_2(\delta_1) = -2s,\\
&(6+s)b_3 + d_3'\left(-\delta_1^2 - 4 - (2+s)\Delta_3(\delta_1) + \frac{\delta_1^4}{\lambda^2}\right)\\
&\qquad + c_3'\left(-\Gamma_1^2 - 4 - (2+s)\Delta_3(\Gamma_1) + \frac{\Gamma_1^4}{\lambda^2}\right) = -2s,\\
&-6b_1 + d_1'\left(-\delta_1^2 - 4 - 2\Delta_1(\delta_1) + \frac{\delta_1^4}{\lambda^2}\right)\\
&\qquad + c_1'\left(-\Gamma_1^2 - 4 - 2\Delta_1(\Gamma_1) + \frac{\Gamma_1^4}{\lambda^2}\right)\\
&\qquad - \mu d_2'\left(-\delta_1^2 - 4 - 2\Delta_2(\delta_1) + \frac{\delta_1^4}{\lambda^2}\right) + 6\mu c_2 = 0,\\
&d_1'\delta_1^2\{\Delta_1(\delta_1) + (1+e)\} + c_1'\Gamma_1^2\{\Delta_1(\Gamma_1) + (1+e)\} = 0,\\
&-d_2'\delta_1^2\{\Delta_2(\delta_1) + (1+e) + c_2\{10 - 10e\} = 0,\\
&d_3'\delta_1^2\{\Delta_3(\delta_1) + (1+e)\} + c_3'\Gamma_1^2\{\Delta_3(\Gamma_1) + (1+e)\} = 0,
\end{aligned} \tag{3.15}$$

where

$$d_1' = d_1K_{\frac{3}{2}}(\delta_1),\ c_1' = c_1K_{\frac{3}{2}}(\Gamma_1),\ d_2' = d_2I_{\frac{3}{2}}(\delta_1),\ d_3' = d_3K_{\frac{3}{2}}(\delta_1),\ c_3' = c_3K_{\frac{3}{2}}(\Gamma_1).$$

Solving the above equations, we get:

$$
\begin{aligned}
&b_1 = -1 + (\zeta_1 - 1)c_1', \quad d_1' = -\zeta_1 c_1', \quad c_1' = \frac{-(3s+6)n_5' + 6m_5'}{Z_1},\\
&b_2 = -(\zeta_2 + 1)d_2', \quad c_2 = \zeta_2 d_2', \quad d_2' = \frac{(3s+6)n_4' - 6m_4'}{Z_1},\\
&b_3 = -1 + (\zeta_3 - 1)c_3', \quad d_3' = -\zeta_3 c_3', \quad c_3' = \frac{-(3s+6)}{n_3'},\\
&\zeta_1 = \frac{\Gamma_1^2[\Delta_1(\Gamma_1) + (1+e)]}{\delta_1^2[\Delta_1(\delta_1) + (1+e)]}, \quad \zeta_2 = \frac{\delta_1^2[\Delta_2(\delta_1) + (1+e)]}{(10 - 10e)},\\
&\zeta_3 = \frac{\Gamma_1^2[\Delta_3(\Gamma_1) + (1+e)]}{\delta_1^2[\Delta_3(\delta_1) + (1+e)]},
\end{aligned}
\tag{3.16}
$$

where $Z_1 = m_4' n_5' - m_5' n_4'$ and

$$
\begin{aligned}
m_4' &= \left[\zeta_1\left(-2 - s + \delta_1^2 + (2+s)\Delta_1(\delta_1) - \frac{\delta_1^4}{\lambda^2}\right)\right.\\
&\quad \left. + s + 2 - \Gamma_1^2 - (2+s)\Delta_1(\Gamma_1) + \frac{\Gamma_1^4}{\lambda^2}\right],\\
m_5' &= s[-2\zeta_2 + 2 + \Delta_2(\delta_1)],\\
n_4' &= \left[\zeta_1\left(-2 + \delta_1^2 + 2\Delta_1(\delta_1) - \frac{\delta_1^4}{\lambda^2}\right) + 2 - \Gamma_1^2 - 2\Delta_1(\Gamma_1) + \frac{\Gamma_1^4}{\lambda^2}\right],\\
n_5' &= \mu\left[6\zeta_2 + \delta_1^2 + 4 + 2\Delta_2(\delta_1) - \frac{\delta_1^4}{\lambda^2}\right],\\
n_3' &= \left[\zeta_3\left(-2 - s + \delta_1^2 + (2+s)\Delta_3(\delta_1) - \frac{\delta_1^4}{\lambda^2}\right)\right.\\
&\quad \left. + s + 2 - \Gamma_1^2 - (2+s)\Delta_3(\Gamma_1) + \frac{\Gamma_1^4}{\lambda^2}\right].
\end{aligned}
\tag{3.17}
$$

Thus, outside and inside flows of stream functions are found.

3.2. Drag force evaluation

A fluid sphere submerged in CSF fluid experiences the drag force, which is equal to:

$$
D_{g2} = 2\pi a^2 \int_{\theta=0}^{\pi} [\tau_{rr}\cos\theta - \tau_{r\theta}\sin\theta]_{r=1}\sin\theta\, d\theta. \tag{3.18}
$$

With $x = \cos\theta$ and $x_0 = \cos(\theta_0)$ as a cap angle. Substituting Eqs. (3.16), (3.17) and simplifying, we obtained the drag force with a cap angle as:

$$
\begin{aligned}
(3.19)\qquad D_{g2} = -2\pi a\mu_e U_\infty \Bigg\{ & \left[\Gamma_1^2 - \frac{\Gamma_1^2}{2} b_1 + 4f_{en}(1) - 2f'_{en}(1)\right]\left[\frac{x_0^3}{3} + \frac{1}{3}\right] \\
& + \left[\Gamma_1^2 - \frac{\Gamma_1^2}{2} b_3 + 4f_{ec}(1) - 2f'_{ec}(1)\right]\left[\frac{1}{3} - \frac{x_0^3}{3}\right] \\
& + \left[-f''_{en}(1) + 2f'_{en}(1) + \frac{1}{\delta_1^2} f^{iv}_{en}(1)\right]\left[\frac{x_0}{2} - \frac{x_0^3}{6} + \frac{1}{3}\right] \\
& + \left[\left(1 + \frac{6}{\delta_1^2}\right) f_{en}(1) - \frac{4}{\delta_1^2} f'_{en}(1) + \frac{2}{\delta_1^2} f''_{en}(1)\right]\left[\frac{x_0^3}{3} - x_0 - \frac{2}{3}\right] \\
& + \left[-f''_{ec}(1) + 2f'_{ec}(1) + \frac{1}{\delta_1^2} f^{iv}_{ec}(1)\right]\left[\frac{1}{3} - \frac{x_0}{2} + \frac{x_0^3}{6}\right] \\
& + \left[\left(1 + \frac{6}{\delta_1^2}\right) f_{ec}(1) - \frac{4}{\delta_1^2} f'_{ec}(1) + \frac{2}{\delta_1^2} f''_{ec}(1)\right]\left[-\frac{2}{3} - \frac{x_0^3}{3} + x_0\right]\Bigg\}.
\end{aligned}
$$

The values in Eqs. (3.6) and (3.8) are taken on R.H.S. to calculate Eq. (3.19).

When $x_0 = -1$, a contaminated fluid sphere reduces to a solid sphere. Then drag Eq. (3.19) becomes

$$
\begin{aligned}
(3.20)\qquad D_{g2} = -2\pi a\mu_e U_\infty \Bigg\{ & \left[\frac{2}{3}\right]\left[\Gamma_1^2 - \frac{\Gamma_1^2}{2} b_3 + 4f_{ec}(1) - 2f'_{ec}(1)\right] \\
& + \left[\frac{2}{3}\right]\left[-f''_{ec}(1) + 2f'_{ec}(1) + \frac{1}{\delta_1^2} f^{iv}_{ec}(1)\right] \\
& - \left[\frac{4}{3}\right]\left[\left(1 + \frac{6}{\delta_1^2}\right) f_{ec}(1) - \frac{4}{\delta_1^2} f'_{ec}(1) + \frac{2}{\delta_1^2} f''_{ec}(1)\right]\Bigg\}.
\end{aligned}
$$

When $x_0 = 1$, the contaminated fluid sphere reduces to a fluid sphere. Then Eq. (3.19) becomes

$$
\begin{aligned}
(3.21)\qquad D_{g2} = -2\pi a\mu_e U_\infty \Bigg\{ & \left[\frac{2}{3}\right]\left[\Gamma_1^2 - \frac{\Gamma_1^2}{2} b_1 + 4f_{en}(1) - 2f'_{en}(1)\right] \\
& + \left[\frac{2}{3}\right]\left[-f''_{en}(1) + 2f'_{en}(1) + \frac{1}{\delta_1^2} f^{iv}_{en}(1)\right] \\
& - \left[\frac{4}{3}\right]\left[\left(1 + \frac{6}{\delta_1^2}\right) f_{en}(1) - \frac{4}{\delta_1^2} f'_{en}(1) + \frac{2}{\delta_1^2} f''_{en}(1)\right]\Bigg\}.
\end{aligned}
$$

Substituting values obtained from Eqs. (3.16), (3.17) with the assumption of $\Gamma_1^2 = 0$ (no porosity), the couple stress parameter ($\delta_1^2 \to \infty$) and $s \to \infty$ (the slip condition reduces to a no-slip condition), we obtained the drag force for a solid sphere with no slip condition as

$$
(3.22)\qquad D_{g2} = 6\pi a\mu_e U_\infty
$$

which matches with the results of DEO *et al.* [17], HAPPEL and BRENNER [30], SWAN and KHAIR [42]).

Now the coefficient of drag (C_D) is computed as:

$$C_D = \frac{D_{g2}}{\frac{1}{2}\pi\rho U_\infty^2 a^2} = \frac{\pi\mu_e U a \Gamma_1^2(-2 - c_1' - c_3' - d_1' - d_3')}{\frac{1}{2}\pi\rho U_\infty^2 a^2}. \tag{3.23}$$

When $s \to \infty$, $\mu \to \infty$, $\delta_1^2 \to \infty$ and $\Gamma_1 = 0$, then we get:

$$C_D = -\frac{24}{Re}, \quad \text{with } Re = \frac{(2a)\rho U_\infty}{\mu_e}, \tag{3.24}$$

which matches with the coefficient of drag (C_D) for a solid sphere without the slip condition (HAPPEL and BRENNER [30]).

4. Results and discussion

We obtained stream function for internal and external flows to the spherical cap. Then the drag acts on a spherical cap due to the external flow by using an integral formula on the stream function. Here two cases of flows past the contaminated sphere are considered. 1. The viscous flow past the viscous contaminated fluid sphere and 2. The couple stress fluid past the couple stress fluid contaminated sphere. In both cases, the effect of physical parameters on the drag are shown in the form of figures.

Case 1: The uniform viscous fluid flow past a contaminated viscous fluid sphere in a porous medium:

i) The numerical results of the coefficient of the drag (C_D) for the differing porosity parameter (Γ), the viscosity ratio (μ)at the fixed slip parameter (s) for

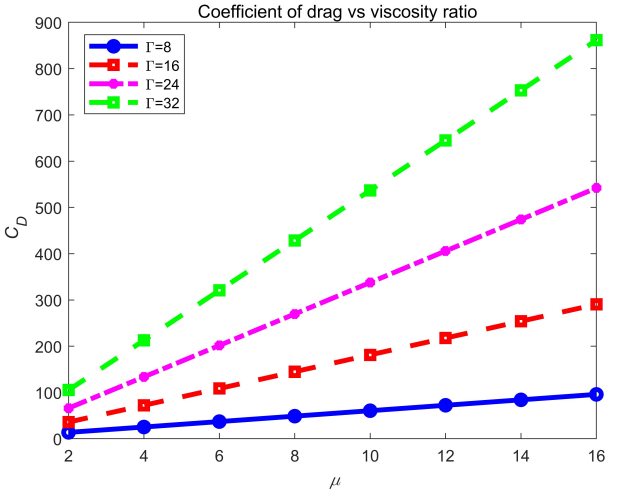

FIG. 3. The coefficient of drag (C_D) for viscous fluid w.r.t. viscosity ratio (μ) for varying porosity parameter (Γ) at a fixed slip parameter (s) = 5, cap value $x_0 = 0$.

TABLE 1. The coefficient of drag (C_D) for viscous fluid w.r.t. viscosity ratio (μ) for varying porosity parameter (Γ) at a fixed slip parameter (s) = 5, cap value $x_0 = 0$.

μ	Γ			
	8	16	24	32
2	13.7459	35.9803	66.0365	105.2451
4	25.3372	72.2851	133.7216	212.7528
6	37.0578	108.6189	201.6537	320.6603
8	48.8064	144.9614	269.6692	428.7095
10	60.5656	181.3077	337.7229	536.8249
12	72.3300	217.6559	405.7971	644.9767
14	84.0973	254.0053	473.8837	753.1506
16	95.8664	290.3555	541.9784	861.3390

Eq. (2.21) at an assumed cap value $x_0 = 0$ are plotted in Fig. 3 and tabulated in Table 1, respectively. It is noticed that as the viscosity ratio (μ) value rises the coefficient of drag (C_D) also rises. This is because that as (μ) increases, the viscosity for internal fluid increases and hence the friction resistance of internal fluid increases and hence the drag increases.

ii) The numerical results of the coefficient of drag (C_D) for differing slip parameter (s), the porosity parameter (Γ) at the fixed viscosity ratio (μ), are plotted for Eq. (2.21) at an assumed cap value $x_0 = 0$ and tabulated in Fig. 4 and Table 2, respectively. It was noticed that as the porosity parameter value (Γ)

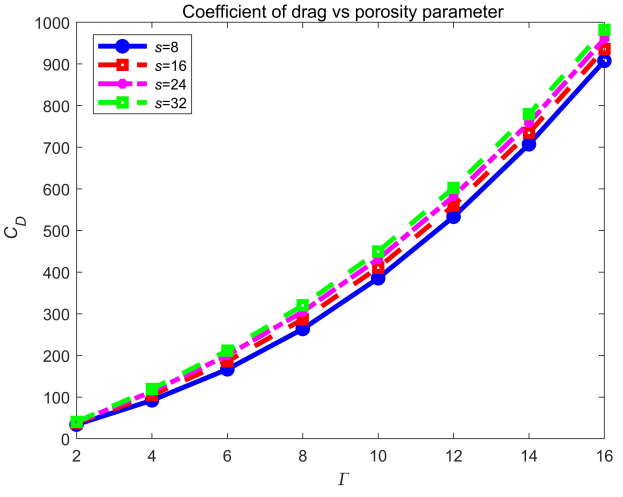

FIG. 4. The coefficient of drag(C_D)for viscous fluid w.r.t. porosity parameter (Γ) for varying slip parameter (s) at fixed value $\mu = 5$, cap value $x_0 = 0$.

TABLE 2. The coefficient of drag (C_D) for viscous fluid w.r.t. porosity parameter (Γ) for varying slip parameter (s) at fixed value $\mu = 5$, cap value $x_0 = 0$.

Γ	s			
	8	16	24	32
2	34.0014	37.5536	39.4587	40.6469
4	92.2715	105.0179	113.3793	119.2966
6	166.7316	186.1232	200.5041	211.6837
8	263.6211	286.8170	305.2266	320.4025
10	385.4661	410.8650	431.8227	449.7321
12	533.1957	559.9422	582.5415	602.2994
14	707.1922	734.8102	758.5060	779.5376
16	907.6320	935.8414	960.2973	982.2304

rises the coefficient of drag (C_D) also rises. This is because as (Γ) increases, the value of k decreases and hence the fluid behaves like a solid which means that the permeability of the medium decreases. Hence the fluid requires more force to pass through the medium and hence the drag increases.

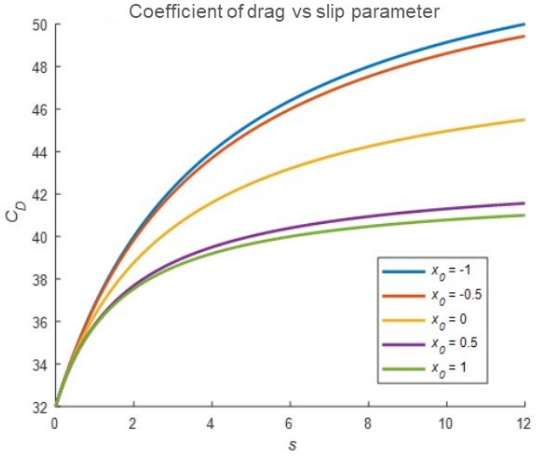

FIG. 5. The coefficient of drag (C_D) for viscous fluid for varying slip parameter (s), varying cap value (x_0) at a fixed value viscosity ratio (μ) = 1, porosity parameter (Γ) = 1.

iii) The numerical results of the coefficient of drag (C_D) for the differing slip parameter (s), the cap angle (x_0) at the fixed viscosity ratio (μ), the porosity value is plotted for Eq. (2.21) Fig. 5. It was noticed that as the slip parameter value (s) rises the coefficient of drag (C_D) also increases.

Case 2: the uniform flow of CSF past a contaminated CSF sphere in a porous medium:

The inside and outside stream functions of Eq. (3.6) to Eq. (3.9) are calculated using the BC's from (3.10)–(3.14). The drag force (D_{g2}) of CSF past a contaminated CSF in a porous medium with slip conditions computed as given in Eq. (3.19).

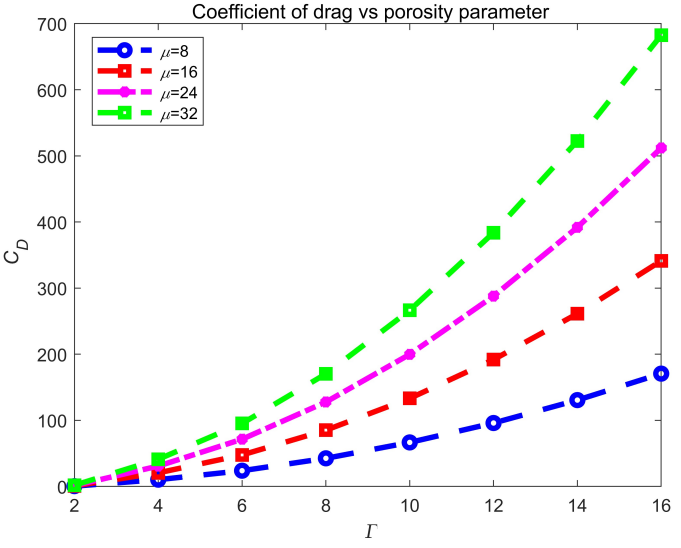

FIG. 6. The coefficient of drag (C_D) for CSF w.r.t porosity parameter (Γ) for varying viscosity ratio (μ) at fixed $s = 5$, $e = 2$, cap value $x_0 = 0$.

The numerical results of the coefficient of drag (C_D) for the differing viscosity ratio (μ), the porosity parameter (Γ) at the fixed slip parameter (s) and the couple stress parameter (e) are plotted for Eq. (3.19) a cap value $x_0 = 0$ and tabulated in Fig. 6 and Table 3, respectively. It was noticed that as the porosity

TABLE 3. The coefficient of drag (C_D) for CSF w.r.t. porosity parameter (Γ) for varying viscosity ratio (μ) at fixed $s = 5$, $e = 2$, cap value $x_0 = 0$.

Γ	μ			
	8	16	24	32
2	0.4872	0.9193	1.3503	1.7810
4	10.2830	20.5622	30.8414	41.1205
6	23.8324	47.6640	71.4956	95.3273
8	42.5727	85.1452	127.7176	170.2901
10	66.6066	133.2131	199.8196	266.4261
12	95.9583	191.9166	287.8748	383.8331
14	130.6360	261.2721	391.9081	522.5441
16	170.6432	341.2864	511.9296	682.5728

parameter value (Γ) increases the coefficient of drag (C_D) also rises. This is because as (Γ) increases, the value of k decreases and hence the fluid behaves like a solid which means that the permeability of the medium decreases. Hence the fluid requires more force to pass through the medium and hence the drag increases.

Case 3: the numerical results of the coefficient of drag (C_D) for the fixed porosity parameter ($\Gamma = 8$), the slip parameter (s) at the fixed viscosity ratio (μ) and the couple stress parameter (e) are plotted and tabulated in Fig. 7 and Table 4. It is noticed that for viscous fluid flow, with a rise in slip parameter rises (s) values, the coefficient of drag (C_D) also rises and for CSF fluid flow, with a rise in slip parameter (s) the coefficient of drag (C_D) decreases. Also observed that with couple stress fluid flows the coefficient of drag values are lower than the viscous fluid flow. This is because shear stress contains terms from couple stress components, which will decrease the effect of shear force.

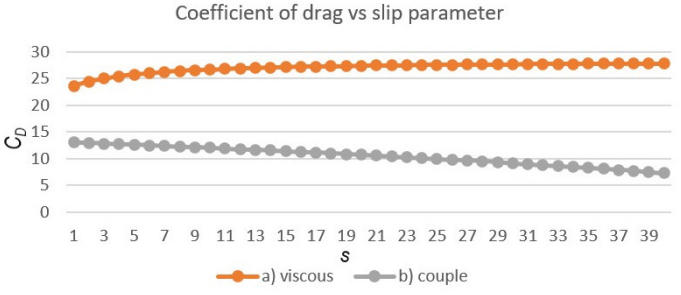

FIG. 7. a) Viscous coefficient of drag (C_D) and b) couple stress coefficient of drag (C_D) w.r.t. (s) slip parameter for fixed porosity parameter ($\Gamma = 8$) at fixed $\mu = 5$, $e = 2$.

TABLE 4. a) viscous coefficient of drag (C_D) and b) couple stress coefficient of drag (C_D) w.r.t. (s) slip parameter for fixed porosity parameter ($\Gamma = 8$) at fixed $\mu = 5$, $e = 2$.

C_D	s								
	1	5	10	15	20	25	30	35	40
a	23.5739	25.7267	26.6606	27.0987	27.3532	27.5196	27.6368	27.7239	27.7911
b	13.0239	12.5897	12.0088	11.3805	10.699	9.9569	9.1459	8.256	7.2748

5. Conclusions

In this study, we acquired an analytical solution for a uniform flow of the CSF flow over a contaminated couple stress fluid sphere placed in a porous medium with the slip condition on its surface. In addition, an exact solution of viscous fluid flow through a contaminated sphere of viscous fluid is also obtained. The

internal and external stream functions, as well as the drag force for above cases were computed analytically. Results of special cases for the non-porous medium of a solid sphere without the slip condition, i.e., when $s \to \infty$, solid sphere when $\mu \to \infty$, no porous region, i.e., $\Gamma_1 = 0$ are reduced, which is consistent with data in literature.

It was observed that:

- In viscous fluid and couple stress fluid cases with an increase in the viscosity ratio, the slip parameter (s), the porous parameter there is an increase in the coefficient of drag values.
- The coefficient of drag values for a uniform flow of the viscous fluid over a contaminated viscous fluid sphere in a porous medium with the slip condition is superior to that of a CSF flow.

The above findings will help for further study with other non-Newtonian fluids with no-slip or slip or stress jump conditions, heat and mass transfer, MHD effects, etc., which have physical applications in biological research in industry.

Acknowledgments

The article was substantially enhanced by the corrections suggested by the referee(s), for which the authors are grateful.

References

1. K. KUMAR, V. SINGH, S. SHARMA, *On the onset of convection in a dusty couple-stress fluid with variable gravity through a porous medium in hydro magnetics*, Journal of Applied Fluid Mechanics, **8**, 1, 55–63, 2015.
2. D. SRINIVASACHARYA, J.V. RAMANA MURTHY, *Flow past an axisymmetric body embedded in a saturated porous medium*, Comptes Rendus Mécanique, **330**, 417–423, 2002.
3. G.E. PAVLOVSKAYA, T. MEERSMANN, CH. JIN, S.P. RIGBY, *Fluid flow in a porous medium with transverse permeability discontinuity*, Physical Review Fluids, **3**, 4, 1–20, 2018.
4. H.C. BRINKMAN, *A calculation of the viscous force exerted by a flowing fluid on a dense swarm of particles*, Journal of Applied Sciences Research, 27–34, 1947.
5. M.K. PARTHA, P.V.S.N. MURTHY, G.P.R. SEKHAR, *Viscous flow past a porous spherical shell-effect of stress jump boundary condition*, Journal of Engineering Mechanics, **131**, 1291–1301, 2005.
6. T.S.L. RADHIKA, T.K.V. IYENGAR, *Stokes flow of an incompressible couple stress fluid past a porous spheroidal shell*, Proceedings of the International Multi Conference of Engineers and Computer Scientists, **3**, 1–7, 2010.
7. H. ALEMAYEHU, G.R. KRISHNAMACHARYA, *Dispersion of a solute in peristaltic motion of a couple stress fluid through a porous medium with slip condition*, World Academy of Science Engineering and Technology, **51**, 803–808, 2011.

8. P. Kumar, *Thermo solutal magneto – rotatory convection in couple – stress fluid through porous medium*, Journal of Applied Fluid Mechanics, **5**, 4, 45–52, 2012.
9. P. Kumar, H. Mohan, *Convection in couple-stress rotatory-fluid through porous medium*, Science International, **5**, 2, 47–55, 2017.
10. B.M. Agoor, N.T.M. Eldabe, *Rayleigh–Taylor instability at the interface of superposed couple-stress Casson fluids flow in porous medium under the effect of a magnetic field*, Journal of Applied Fluid Mechanics, **7**, 4, 573–580, 2014.
11. G. Nagaraju, A. Matta, P. Aparna, *Heat transfer on the MHD flow of couple stress fluid between two concentric rotating cylinders with porous lining*, International Journal of Advances in Applied Mathematics and Mechanics, **3**, 1, 77–86, 2015.
12. N. Rudraiah, K.S. Mallika, N. Sujatha, *Electrohydrodynamic dispersion with interphase mass transfer in a poorly conducting couple stress fluid bounded by porous layers*, Journal of Applied Fluid Mechanics, **9**, 1, 71–81, 2016.
13. A.R. Hassan, S.O. Adesanya, R.S. Lebelo, J.A. Falade, *Irreversibility analysis for a mixed convective flow of a reactive couple stress fluid flow through channel saturated porous materials*, International Journal of Heat and Technology, **35**, 3, 633–638, 2017.
14. L.E. Howle, R.P. Behringer, J.G. Georgiads, *Convection and flow in porous media. Part 2. Visualization by shadowgraph*, Journal of Fluid Mechanics, **332**, 247–262, 1997.
15. D. Srinivasacharya, *Motion of a porous sphere in a spherical container*, Comptes Rendus Mécanique, **333**, 612–616, 2005.
16. D. Srinivasacharya, M.K. Prasad, *Creeping flow past a porous approximate sphere stress jump boundary condition*, Journal of Applied Mathematics and Mechanics, **91**, 10, 824–831, 2011.
17. S. Deo, P. Shukla, B.R. Gupta, *Drag on a fluid sphere embedded in a porous medium*, Advances in Theoretical and Applied Mechanics, **3**, 1, 45–52, 2010.
18. B. Widodo, M. Abu, Ch. Imron, *Unsteady nano fluid flow through magnetic porous sphere under the influence of mixed convection*, 9th International Conference on Physics and its Applications (ICOPIA) IOP, Conference Series: Journal of Physics, **1153,** 1–6, 2019.
19. R. Selvi, P. Shukla, A.N. Filippov, *Flow around a liquid sphere filled with a non-Newtonian liquid and placed into a porous medium*, Colloid Journal, **82**, 152–160, 2020.
20. S.S. Sadhal, P.S. Ayyaswamy, J.N. Chung, *Transport Phenomena with Drops and Bubbles*, Springer, New York, 1997.
21. S.H. Lee, R.S. Chadwick, L.G. Leal, *Motion of a sphere in the presence of a plane interface. Part 1. An approximate solution by generalization of the method of Lorentz*, Journal of Fluid Mechanics, **93**, 4, 705–726, 1979.
22. H.N. Oguz, S.S. Sadhal, *Effects of soluble and insoluble surfactants on the motion of drops*, Journal of Fluid Mechanics, **194**, 563–579, 1988.
23. D.T. Wasan, *Structure and Dynamics of Thin Liquid Films*, Interfacial Transport Processes and Rheology – Chemical Engineering Education, pp. 104–111, 1992.
24. A. Saboni, S. Alexandrova, M. Karsheva, Ch. Gourdon, *Mass transfer from a contaminated fluid sphere*, AIChE Journal, **57**, 7, 1684–1692, 2011.
25. J.V.R. Murthy, M.P. Kumar, *Exact solution for flow over a contaminated fluid sphere for Stokes flow*, Journal of Physics: Conference Series, **662**, 012016, 2015.
26. C.L.M.H. Navier, *Mémoire sur les lois du Mouvement des Fluides*, Mémoires de l'Académie Royale des Sciences de l'Institut de France, 389–440, 1823.

27. O.I. VINOGRADOVA, *Drainage of a thin liquid film confined between hydrophobic surfaces*, Langmuir, **11**, 6, 2213–2220, 1995.

28. C.O. NG, *How does wall slippage affect hydrodynamic dispersion*, Microfluidics and Nanofluidics, **10**, 47–57, 2011.

29. Z.-G. FENG, E.E MICHAELIDES, S. MAO, *On the drag force of a viscous sphere with interfacial slip at small but finite Reynolds numbers*, Fluid Dynamics Research, **44**, 025502, 1–16, 2012.

30. J. HAPPEL, H. BRENNER, *Low Reynolds Number Hydrodynamics*, Martinus Nijhoff publishers, The Hague, 1983.

31. E.E. MICHAELIDES, *Particles, Bubbles and Drops – Their Motion, Heat and Mass Transfer*, World Scientific Publishing, 2006.

32. J.V.R. MURTHY, M.P. KUMAR, *Effect of slip parameter on the flow of viscous fluid past an impervious sphere*, International Journal of Applied Science and Engineering, **12,** 203–223, 2014.

33. P.N.L. DEVI, M.P. KUMAR, *Drag over a fluid sphere filled with couple stress due to flow of a couple stress fluid with slip condition*, Trends in Sciences, **19**, 24, 3133, 2022.

34. P.N.L. DEVI, M.P. KUMAR, *Couple stress fluid past a contaminated fluid sphere with slip condition*, Applied Mathematics and Computation, **446**, 1–12, 2023.

35. P.N.L. DEVI, M.P. KUMAR, *Oscillatory flow of couple stress fluid flow over a contaminated fluid sphere with slip condition*, CFD Letters, **15**, 8, 148–165, 2023.

36. K.V. LAKSHMI, M.P. KUMAR, *Stokes flow on micropolar fluid beyond fluid sphere with slip condition*, Journal of Applied Mathematics and Mechanics, **102**, 1–11, 2022.

37. K.V. LAKSHMI, M.P. KUMAR, *Exact solution for non-Newtonian fluid flow beyond a contaminated fluid sphere*, Engineering Transactions, **70**, 3, 287–299, 2022.

38. P. DEBYE, A.M. BUECHE, *Intrinsic viscosity, diffusion, and sedimentation rate of polymers in solution*, Journal of Chemical Physics, **16**, 573, 573–579, 1948, doi: 10.1063/1.1746948.

39. K. DANOV, R. AUST, F. DURST, U. LANGE, *Influence of the surface viscosity on the hydrodynamic resistance and surface diffusivity of a large Brownian particle*, Journal of Colloid and Interface Science, **175**, 36–45, 1995.

40. V. CRISTINI, J. BŁAWZDZIEWICZ, M. LOEWENBERG, *Drop breakup in three-dimensional viscous flows*, Physics Fluids, **10**, 8, 1781–1783, 1998.

41. H.A. STONE, A.D. STROOCK, A. AJDARI, *Engineering flows in small devices: microfluidics toward a lab-on-a-chip*, Annual Review of Fluid Mechanics, **36**, 381–411, 2004.

42. J.W. SWAN, A.S. KHAIR, *On the hydrodynamics of 'slip–stick' spheres*, Journal of Fluid Mechanics, **606**, 115–132, 2008.

43. V.K. STOKES, *Couple stresses in fluids*, Physics of Fluids, **9**, 1710–1715, 1966.

Received August 11, 2023; revised version April 1, 2024.
Published online June 21, 2024.